

# 1 **Reconstructing the phylodynamic history and geographic spread of the** 2 **CRF01\_AE-predominant HIV-1 epidemic in the Philippines from PR/RT** 3 **sequences sampled from 2008-2018**

4  
5 Francisco Gerardo M. Polotan <sup>1\*</sup>, Carl Raymund P. Salazar<sup>2</sup>, Hannah Leah E. Morito<sup>3</sup>, Miguel Francisco B.  
6 Abulencia<sup>1</sup>, Roslind Anne R. Pantoni<sup>1</sup>, Edelwisa S. Mercado<sup>1</sup>, Stéphane Hue<sup>4,5&</sup>, Rossana A. Ditangco<sup>1&</sup>

7  
8 <sup>1</sup>Research Institute for Tropical Medicine, Muntinlupa City, Philippines

9 <sup>2</sup>Laboratory of Microbiology, Wageningen University and Research, Wageningen, The Netherlands

10 <sup>3</sup>Medizinische Hochschule Hannover, Hannover, Germany

11 <sup>4</sup>Centre for the Mathematical Modelling of Infectious Diseases (CMMID), London School of Hygiene &  
12 Tropical Medicine, London, UK

13 <sup>5</sup>Department of Infectious Disease Epidemiology, London School of Hygiene & Tropical Medicine, London,  
14 UK

15  
16 &SH and RD contributed equally

17 \*corresponding author

18 Email: fgmpolotan@gmail.com

## 19 20 **Abstract**

21 The Philippines has had a rapidly growing HIV epidemic with a shift in the prevalent subtype  
22 from B to CRF01\_AE. However, the phylodynamic history of CRF01\_AE in the Philippines  
23 has yet to be reconstructed. We conducted a descriptive retrospective study reconstructing the  
24 history of HIV-1 CRF01\_AE transmissions in the Philippines through molecular  
25 epidemiology. Partial polymerase sequences ( $n = 1429$ ) collected between 2008 and 2018  
26 from 13 Philippine regions were collated from the RITM drug resistance genotyping database.  
27 Subsampling was performed on these Philippine and Los Alamos National Laboratory HIV  
28 international sequences followed by estimation of the time to the most recent common  
29 ancestor (tMRCA), effective reproductive number ( $R_e$ ), effective viral population size ( $N_e$ ),  
30 relative migration rates and geographic spread of CRF01\_AE with BEAST.  $R_e$  and  $N_e$  were  
31 compared between CRF01\_AE and B. Most CRF01\_AE sequences formed a single clade with  
32 a tMRCA of 1999 [95% HPD: 1996, 2001]. Exponential growth of  $N_e$  was observed from  
33 1999 to 2013. The  $R_e$  reached peaks of 3.71 [95% HPD: 1.71, 6.14] in 2009 and 2.87 [95%  
34 HPD: 1.78, 4.22] between 2012 and 2015. A transient decrease to 0.398 [95% HPD: 0.0105,  
35 2.28] occurred between 2010 and 2012. The epidemic most likely started in Luzon in the  
36 National Capital Region, which then spread diffusely to the rest of the country. Both  
37 CRF01\_AE and subtype B exhibited similar but unsynchronized patterns of  $R_e$  over time.  
38 These results characterize the subtype-specific phylodynamic history of the CRF01\_AE  
39 epidemic in the Philippines, which contextualizes and may inform past, present, and future  
40 public health measures toward controlling the HIV epidemic in the Philippines.

41  
42 **Running Title:** HIV-1 subtype CRF01\_AE phylodynamics in the Philippines

43 **Keywords:** HIV-1, epidemic, CRF01\_AE, subtype B, phylodynamics, molecular  
44 epidemiology, Philippines

## 45 **Introduction**

46 Human immunodeficiency virus-1 (HIV-1) infections and deaths related to acquired  
47 immunodeficiency syndrome (AIDS) have been rapidly increasing in the Philippines over  
48 the past years, with a 237% percent change in new infections, the highest in Asia and the  
49 Pacific from 2010 to 2020 [1]. As of June 2022, 101,768 confirmed HIV cases have been  
50 reported since January 1984, with about 92% of these reported in the last 10 years and the  
51 number of new diagnoses increasing from 6 cases/day in 2011 to 41 cases/day in 2022 [2].

52 The demographics of HIV-1 cases in the Philippines have also shifted over time.  
53 From 1984 to 1990, the majority of diagnosed cases (62%) were females, compared to a  
54 majority of male cases (94%) in 1991–2020 [3]. The largest proportion of new cases also  
55 shifted to a younger age group, from 35–49 in 2001–2005 to 25–34 and 15–24 age groups  
56 in 2010–2022 [2], [4], [5], [6]. Furthermore, the majority of transmissions were from male-  
57 to-female sex until 2009, pointing to sexually active men who have sex with men (MSM) as  
58 the major transmitters of HIV-1 in the Philippines since 2010 [5].

59 The composition of circulating subtypes in the Philippines has also changed. In  
60 1998, the major subtype was B, with around 70% of infections, followed by the  
61 CRF01\_AE, a putative recombinant of subtypes A and E, with 16–29% of infections [7],  
62 [8]. However, the major subtype has shifted to CRF01\_AE, making up 77% of HIV-1  
63 patients in a 2013 cohort and with 22% of the same cohort being subtype B [8]. A more  
64 recent cohort from 2016 to 2018 reported the distribution of 77% CRF01\_AE, 13.8%  
65 subtype B, and 9.2% other subtypes or recombinants [9]. Furthermore, CRF01\_AE was the  
66 major subtype among the MSM population, while B was predominant among injecting drug  
67 users (IDUs) in infections from 2007 to 2012 [10], [11]. It is important to highlight that the

68 HIV epidemic in the Philippines is predominantly CRF01\_AE, which displays high  
69 antiretroviral resistance [12], and thus treatment regimens may need readjustment since  
70 recommendations are based primarily on clinical trials from regions with subtype B  
71 infections [13], [14].

72 CRF01\_AE may have been introduced into the Philippines around the mid-1990s,  
73 potentially from a neighboring Asian or Southeast Asian country [15], [16]. Despite the  
74 predominance of CRF01\_AE among the circulating subtypes in the Philippines, to the best  
75 of our knowledge, there has not yet been any study disentangling epidemiological  
76 parameters of specific HIV subtypes in the Philippines using phylodynamic methods.

77 Although whole genome sequences would be able to more accurately distinguish  
78 recombinant sequences [17] and lead to more precise estimates [18], partial *pol* sequences  
79 from drug resistance genotyping (DRG) have been shown sufficient to reconstruct  
80 transmission histories phylogenetically and are highly available data from routine testing  
81 [19]. The Research Institute for Tropical Medicine (RITM) DRG database has archived *pol*  
82 protease/reverse transcriptase (PR/RT) sequences from routine testing for over a decade  
83 from referred samples spanning multiple Philippine regions, compiling a suitable and  
84 available dataset for reconstructing subtype-specific phylodynamics.

85 Thus, we aimed to reconstruct CRF01\_AE spatiotemporal dynamics using  
86 phylogenetic analysis of available partial *pol* sequences consisting of the PR/RT regions  
87 collected from patient samples referred to the RITM, one of the largest referral hubs in the  
88 Philippines, between 2008 and 2018. We investigated the dates of introduction events;  
89 historical changes in epidemiological parameters of effective viral population size, effective  
90 reproductive number, geographical spread, and migration rates of CRF01\_AE; and how

91 these compared with the  $N_e$  and  $R_e$  of subtype B, to distinguish the relative contribution  
92 each subtype has had to the overall HIV epidemic and provide important context to public  
93 health policies attempting to control its spread in the country.

## 94 **Methods**

### 95 **Study population and sample selection**

96 The retrospective study population were HIV-positive cases from the in-house RITM HIV-  
97 1 DRG database with 1530 cases matching the inclusion criteria (see the following section)  
98 for CRF01\_AE analysis, while 265 cases matched the inclusion criteria for the comparative  
99 subtype B analysis. The data included PR/RT Sanger sequences generated from RITM  
100 routine DRG with accompanying information on specimen collection date. Collated data  
101 for CRF01\_AE analysis consisted of sequences from patient samples from RITM and from  
102 referring hospitals and social hygiene clinics from 13 out of 17 administrative regions from  
103 all three Philippine island groups between January 2008 and November 2018. Meanwhile,  
104 data for the subtype B analysis came from RITM patients and patients from referring  
105 hospitals and social hygiene clinics from 10 out of 17 administrative regions from all three  
106 Philippine island groups between February 2014 and February 2020.

107 Demographic data (i.e., sample collection date and requisitioner address as location)  
108 were obtained via request forms. Missing demographic data from the samples were  
109 requested from the Department of Health Epidemiology Bureau. People living with HIV  
110 have unique HIV laboratory test ID numbers, and these were used to obtain data from the  
111 Epidemiology Bureau without using patient names.

112 The Institutional Review Board (IRB) of the Research Institute of Tropical  
113 Medicine waived ethical approval for this study by granting the study protocol a certificate  
114 of exemption from review as it was a retrospective analysis of archived de-identified  
115 routine DRG sequence data and metadata only.

116

### 117 **Subtype classification and sequence alignment**

118 The inclusion criteria used were: all PR/RT *pol* sequences available in the RITM MBL  
119 DRG; sequences from RITM classified as CRF01\_AE or subtype B; sequences at least 500  
120 nucleotides long. The exclusion criteria were: non-CRF01\_AE or non-subtype B sequences  
121 from RITM MBL DRG, sequences less than 500 nucleotides long; Los Alamos National  
122 Laboratory (LANL) HIV Sequence Database [20] sequences without country and year of  
123 sampling information; sequences containing  $\geq 5\%$  ambiguous nucleotides, frameshift  
124 mutations, stop codons, and APOBEC-mediated hypermutations.

125 Thus, partial *pol* sequences from the RITM DRG database ( $n = 1621$ ) were  
126 classified according to HIV subtype (i.e. phylogenetically related strains defined by close  
127 genetic distance with each other) using the Stanford HIV Drug Resistance Database [21]  
128 and HIVdb program (v8.6) [22], and programs COMET [23] and REGA [24] were used to  
129 exclude non-CRF01\_AE and recombinant sequences, respectively. The 10 most closely  
130 related CRF01\_AE *pol* gene sequences (HXB2 coordinates 2253-3233) per input sequence  
131 were also retrieved from the LANL HIV Sequence Database [20] in January 2019 using  
132 HIV-BLAST. LANL sequences ( $n = 454$ ) from 1990 to 2016 with information on the  
133 sampling year and country and without  $> 5\%$  ambiguous nucleotides, frameshift mutations,

134 stop codons, and APOBEC-mediated hypermutations were retrieved. Sequences that  
135 contained frameshift insertions/deletions as determined by HIVdb were excluded. A small  
136 number of sequences that had very few bases in the PR/RT region or had very long  
137 insertions were also excluded. A codon alignment of all remaining sequences was produced  
138 with the Gene Cutter tool from LANL [25]. A 129 bp-long stretch of sequence, spanning  
139 reference HXB2 codon position 96 of the protease gene to codon position 39 of the reverse  
140 transcriptase gene, was removed from the alignment since a majority of the Philippine  
141 sequences in this study contained gaps in this region. Drug resistance-associated codons  
142 were stripped to remove the influence of convergent evolution from drug resistance  
143 mutations [26]. Large overhangs were trimmed using Aliview [27], and sequences from the  
144 same patient were removed, resulting in 1429 sequences.

145         Using similar procedures, high-confidence subtype B sequences were identified ( $n =$   
146 265) for the comparative analysis. The 10 most similar subtype B *pol* sequences per input  
147 sequence were also retrieved from LANL in May 2021 using HIV-BLAST ( $n = 599$ ).  
148 Codon alignment, filtering, and trimming were also performed. Five partial polymerase  
149 sequences each from of subtype A (DQ396400, DQ445119, JQ403028, KX389622, and  
150 MH705133) and subtype C (AB023804, AB097871, AB254143, AB254146, and  
151 AB254150) were included as outgroups, leading to 874 sequences.

152         For both CRF01\_AE and subtype B sequences, collection dates with complete year  
153 and month but not day were imputed to the first day of the month, while collection dates  
154 with complete year only but not month and day were imputed to the first month and day of  
155 the year.

156

157 **Phylodynamic analysis**

158 FastTree2 [28] and IQ-TREE2 [29] were used to reconstruct a maximum likelihood  
159 phylogeny from the full CRF01\_AE alignment, and TempEst2 [30] was used to measure  
160 the temporal signal of the sequence alignment by root-to-tip regression analysis. A manual  
161 subsample of sequences from the largest Philippine clade and international sequences  
162 nearest to the clade ( $n = 200$ ) was used to estimate the time of introduction of CRF01\_AE  
163 into the Philippines based on the time to the most recent common ancestor (tMRCA) of that  
164 clade. Only 200 sequences were selected to reduce computation time. BEAST v2.6.7 [31]  
165 was used to estimate the tMRCA of the CRF01\_AE clade, with a Coalescent Bayesian  
166 Skyline Plot (BSP) tree prior [32], bModelTest [33] set as the nucleotide substitution  
167 model, clock rate prior set to a normal distribution ( $M = 1.5E-3$ ,  $S = 4.9E-4$ ) [34]–[37],  
168 clock rate standard deviation prior to an exponential distribution ( $M = 0.1$ ), and the best-  
169 fitting molecular clock model of either strict or relaxed clock [38] determined by the path  
170 sampling and stepping-stone procedure [39], [40] implemented in BEAST v1.10.4 [41].  
171 Five separate Markov chain Monte Carlo (MCMC) chains were run for 10M states each,  
172 sampling every 1000 states. These were combined and downsampled with LogCombiner  
173 [42] to 10,000 states and trees. TreeAnnotator [42] was used with a 10% burnin to generate  
174 the maximum clade credibility (MCC) tree.

175 To estimate the effective viral population size ( $N_e$ ) and effective reproductive  
176 number ( $R_e$ ) of CRF01\_AE across time, the subset of Philippine sequences belonging to the  
177 large Philippine monophyletic clade was used. Sequences with missing sample collection  
178 dates or location data were excluded from the analysis. Sequences from this clade were  
179 subsampled uniformly (Supplemental File XLSX) across time and geographic location [43],

180 [44] according to island group (i.e., Luzon, Visayas, and Mindanao) and between May 2008  
181 and November 2018. Specifically, the subsampling procedure outlined by Hidano et al was  
182 used [44], producing a subset of 260 sequences. BEAST2 was run with the BSP and Birth-  
183 Death Skyline (BDSKY) Serial [45] tree priors, MCMC chain lengths of 400M and 300M  
184 states, sampling every 40,000 and 30,000 states to estimate  $N_e$  and  $R_e$ , respectively.  
185 bModelTest [33] was selected as the nucleotide substitution model, the clock rate prior set  
186 to as indicated previously, and the best-fitting molecular clock model determined by the  
187 path sampling and stepping-stone procedure. For the BSP analysis, the bPopSizes and  
188 bGroupSizes were both set to the dimension of 5. For the BDSKY analysis, the origin of  
189 the epidemic prior was set to a log normal distribution ( $M=3.4$ ,  $S=0.29$ ), the become  
190 uninfected rate prior to a log normal distribution ( $M = 2.08$ ,  $S = 1.0$ ), the sampling  
191 proportion prior to a normal distribution (mean = 0.004, sigma = 0.001), the reproductive  
192 number prior to a log normal distribution ( $M = 0.0$  in log space,  $S = 1.25$ ), and the  
193 reproductive number dimensions to 10. The MCC tree was generated from trees sampled in  
194 the BDSKY analysis using TreeAnnotator [42] with 10% burnin. The bdskyTools R  
195 package was used to smooth the  $R_e$  estimates over time [46].

196 To compare the CRF01\_AE  $N_e$  and  $R_e$  with those of another circulating subtype that  
197 may reflect similar patterns if non-subtype-specific influences were acting upon their  
198 transmission, an equivalent analysis was done using BEAST2 on the largest subtype B  
199 monophyletic clade identified from a phylogeny reconstructed using IQ-TREE 2. No  
200 subsampling was performed as only 195 sequences sampled from September 2008 to  
201 February 2020 were available in this clade. The same respective priors as CRF01\_AE were  
202 used, with bModelTest [33] selected as a nucleotide substitution model and with the best-



203 fitting molecular clock model also determined by the path sampling and stepping-stone  
204 procedure.

205

## 206 **Phylogeographic analysis**

207 We performed a Slatkin–Maddison test [47] on the FastTree2 phylogeny of all sequences  
208 from the large monophyletic Philippine CRF01\_AE clade to test for significant associations  
209 ( $\alpha = 0.05$ ) between the trait of location (island group and region) and tree topology. We also  
210 tested for significant associations ( $\alpha = 0.05$ ) of island group and tree topology using the  
211 Bayesian Tip-Significance Testing (BaTS) package [48], which calculates the Association  
212 Index (AI), Parsimony Score (PS), and Monophyletic Clade (MC) index statistics, on 1000  
213 downsampled trees from the BSP analysis of uniformly subsampled CRF01\_AE sequences  
214 and 999 null replicates. BEAST v1.10.4 [41] was used for the phylogeographic analysis of  
215 the CRF01\_AE alignment with nucleotide positions and demes set as the first and second  
216 partitions, respectively. Analysis was performed using a strict clock model and a BSP tree  
217 prior. The asymmetric discrete trait substitution model with BSSVS was selected for using  
218 Philippine island groups as demes. The symmetric discrete trait substitution model with  
219 BSSVS was selected for using these island groups from the same subsampled data  
220 converted to Philippine regions (NCR, I, II, III, IV-A, V, VI, VII, IX, X, XI, XII, and XIII)  
221 as demes. SpreaD3 [49] was used to visualize phylogeographic migration at eight different  
222 time points and at both island group and regional levels over a geoJSON map of the  
223 Philippines [50].

224 All other settings besides those stated were left at default values. See complete details  
225 of the models and parameters used for each analysis in the Supplemental File XLSX. An  
226 effective sample size (ESS) of  $\geq 200$  was deemed as satisfactory convergence of the estimated  
227 parameters. The TRACER [51], FigTree [52], and IcyTree [53] software and R packages  
228 “ggtree” [54] and “ggplot2” [55] were used to visualize the results.

## 229 **Results**

### 230 **Introduction of CRF01\_AE to the Philippines in the late 1990s to early 2000s**

231 The majority CRF01\_AE sequences sampled in the Philippines (1150/1185; 97%) belonged  
232 to one large monophyletic clade (Fig. 1a; SH-aLRT, UFBoot branch support: 98.3, 100).  
233 Fewer sequences (35/1185; 3%) were singletons or belonged to smaller clusters of at most  
234 three sequences, suggesting multiple introductions from overseas over time. Furthermore,  
235 the large monophyletic Philippine CRF01\_AE clade contained sequences from the United  
236 States, Japan, Hong Kong, Australia, Great Britain, China, and South Korea, suggesting  
237 transmission to and/or from these countries either directly or involving unsampled  
238 intermediate destinations (Fig. 1a). Root-to-tip linear regression on the full set of sequences  
239 showed a positive correlation between sequence diversity and time of sampling (coefficient  
240 of correlation: 0.74;  $R^2 = 0.55$ ), indicating sufficient temporal signal for further molecular  
241 clock estimations (Fig. 1b). Model selection through path sampling and stepping-stone  
242 procedure on a subsample of 200 sequences indicated greater support for a relaxed  
243 molecular clock over a strict clock. Under this model, the large Philippine cluster from the  
244 subsampled alignment had a mean tMRCA of March 1999 [95% HPD: April 1996,  
245 December] (Fig. 1c). Additionally, the estimated evolutionary rate for this international set

246 of sequences was a mean of  $2.413E-3$  [95% HPD:  $2.0457E-3$ ,  $2.7851E-3$ ] nucleotide  
247 substitutions/site/year.

248

### 249 **The growth of CRF01\_AE in the Philippines**

250 Coalescent BSP analysis was conducted with 260 subsampled sequences from the large  
251 Philippine monophyletic clade. Model selection with path sampling and stepping-stone  
252 procedure indicated greater support for a strict clock over a relaxed clock (Supplemental  
253 File XLSX). The resulting Skyline plot, showing changes of effective population size over  
254 time, revealed an exponential growth phase that lasted about 14 years between 1999 and  
255 2013 whereby  $N_e$  increased by four orders of magnitude (Fig. 2b). The peak of this growth  
256 phase was followed by a stable or plateau phase wherein  $N_e$  remained within the same order  
257 of magnitude from 2013 onwards (Fig. 2b).

258

### 259 **Fluctuations of CRF01\_AE reproductive number from the late 1990s to 2016**

260 Phylodynamic analysis was performed with the same 260 subsampled CRF01\_AE  
261 sequences and the best-fitting strict clock model. Between the late 1990s and 2016, the  
262 confidence intervals of the estimated  $R_e$  of CRF01\_AE in the Philippines spanned 1.0 for  
263 two periods, wherein the epidemic or the number of secondary cases per infected case  
264 remained stable, and was significantly above 1.0 for two periods, during which there was  
265 exponential growth of the epidemic (Fig. 2b). In more detail,  $R_e$  increased from about 1.06  
266 [95% HPD: 0.0210, 3.86] to a peak of about 3.71 [95% HPD: 1.71, 6.14] from February of  
267 2000 to April of 2008, then decreased between 2009 and 2013 to as low as 0.398 [95%

268 HPD: 0.0105, 2.28], and finally rebounded up to about 2.87 [95% HPD: 1.78, 4.22] in  
269 December of 2013, where it remained until 2016, the end of the interval with informative  
270 common ancestor nodes from the dataset (Fig. 2b).

### 271 **Transmission of CRF01\_AE from the National Capital Region to other Philippine** 272 **island groups and regions**

273 The Slatkin–Maddison test performed on all Philippine sequences from the large  
274 CRF01\_AE transmission cluster detected significant clustering of sequences by island  
275 group (96 observed transitions, 109–117 min–max null model transitions;  $p$ -value <0.001)  
276 and by Philippine region (152 observed transitions, 163–171 min–max null model  
277 transitions;  $p$ -value <0.001) (Fig. S1). Similarly, with the BaTS test, significant clustering  
278 by island group was obtained for the AI (7.82–10.45 observed 95% CI, 12.86–15.08 null  
279 95% CI,  $p$ -value <0.001), PS (50.00–58.00 observed 95% CI, 69.33–74.42 null 95% CI,  $p$ -  
280 value <0.001), MC Luzon (11.00–17.00 observed 95% CI, 6.44–10.29 null 95% CI,  $p$ -  
281 value = 0.014), MC Visayas (2.00–3.00 observed 95% CI, 1.21–2.08 null 95%,  $p$ -value =  
282 0.002), and MC Mindanao (4.00–6.00 observed 95% CI, 1.96–3.05 null 95% CI,  $p$ -value =  
283 0.0010) statistics (Table S2).

284 Phylogeographic analysis was performed with the same 260 subsampled  
285 CRF01\_AE sequences and the best-fitting strict clock model. The most likely location of  
286 the root of the CRF01\_AE phylogeny was estimated to be either the Luzon island group  
287 (posterior probability = 1.0) (Fig. 3a) or the NCR administrative division (posterior  
288 probability = 0.9992) (Fig. S2a), implicating these locations as the origin of the CRF01\_AE  
289 epidemic. No significant differences were observed among the estimated relative migration  
290 rates between the three different island groups (Fig. 3b).

291 The reconstructed phylogeographical spread of CRF01\_AE over time indicated low  
292 local spread in NCR (Luzon) around early 2000 during the estimated start of the epidemic  
293 followed by a substantial increase by late 2000 (Fig. 3c and Fig. S2c). The spread of the  
294 strain from NCR to Mindanao (Region XI) can be traced back to the late 2004, while the  
295 spread from NCR to Visayas (Region VI) can be traced back to 2007 (Fig. 3c and Fig.  
296 S2c). Local spread in all three island groups increased by mid-2008 during the peak of  $R_e$   
297 (Fig. 3c and Fig. S2c). When  $R_e$  rebounded during the late 2013 and onward, the strain was  
298 reintroduced to Luzon from Mindanao (Fig. 3c and Fig. S2c).

299

300 **CRF01\_AE effective population size  $N_e$  overtook that of subtype B around 2013, while**  
301 **the effective reproductive number  $R_e$  of the two subtypes fluctuated out of phase**

302 To contextualize the population dynamics of CRF01\_AE, phylodynamic analysis was also  
303 performed on subtype B sequences available in the RITM Molecular Biology Laboratory  
304 database and by using the best-fitting relaxed clock model determined by the path sampling  
305 and stepping-stone procedure (Supplemental File XLSX), focusing on the largest  
306 monophyletic Philippine clade of subtype B sequences (Fig. S3). The resulting BSP  
307 analysis revealed an exponential growth phase in subtype B  $N_e$  from 2003 until about 2010,  
308 during which it was comparable to the CRF01\_AE  $N_e$  (Fig. 4), followed by a peak and  
309 plateau phase wherein  $N_e$  remained within the same order of magnitude from 2010 onwards  
310 (Fig. 4). The CRF01\_AE  $N_e$  had a longer lasting growth phase and a significantly higher  
311 peak than the subtype B  $N_e$  by 2013 (Fig. 4). The estimated evolutionary rate of 2.524E-3  
312 [95% HPD: 1.8829E-3, 3.1806E-3] substitutions/site/year and tMRCA of 1995.1435 [95%

313 HPD: 1982.4503, 2003.6044] for subtype B were not significantly different from those of  
314 CRF01\_AE (Table 1).

315         Phylogenetic analysis with the Birth–Death Skyline Serial model showed that the  
316 trend of the subtype B  $R_e$  also fluctuated over time in a similar but lagging pattern  
317 compared with the  $R_e$  of CRF01\_AE (Fig. 2a; Supplemental File XLSX). During the first  
318 peak of the CRF01\_AE  $R_e$  around 2008 (3.71 [95% HPD: 1.71, 6.14] in 2008-04-10), the  
319 subtype B  $R_e$  was still increasing (1.26 [95% HPD: 0.0225, 3.70] in 2008-01-28) (Fig. 2c).  
320 When the CRF01\_AE  $R_e$  transiently decreased around 2010–2011 (0.398 [95% HPD:  
321 0.0105, 2.28] in 2011-07-16), the subtype B  $R_e$  had reached its first peak phase (2.32 [95%  
322 HPD: 0.86, 4.15] in 2011-07-07) (Fig. 2c). When the CRF01\_AE  $R_e$  rebounded in 2013  
323 (2.87 [95% HPD: 1.78, 4.22] in 2013-12-26), the subtype B  $R_e$  was decreasing (1.63 [95%  
324 HPD: 0.73, 2.48] in 2013-11-30) until it increased again in early 2016 (2.10 [95% HPD:  
325 0.85, 2.96] in 2016-04-25) (Fig. 2c). The peaks and troughs of the subtype B  $R_e$   
326 fluctuations were less in magnitude and steepness than those of CRF01\_AE (Fig. 2c).

## 327 **Discussion**

328 The HIV CRF01\_AE phylogeny in this study revealed a large monophyletic Philippine  
329 clade, supporting a single past introductory event that led to the majority of infections in the  
330 country. This is consistent with the first-comer advantage and strong founder effect  
331 observed in HIV epidemics outside Africa [37]. Based on the phylogeny of sampled  
332 sequences, there is no evidence of much ongoing transmission from other sporadic  
333 introductions. The monophyly and estimated tMRCA of CRF01\_AE are consistent with  
334 results from a study using nearly full-length genomes from the Philippines [15] and a recent  
335 reconstruction of CRF01\_AE transmission from Africa to Asia [16]. The tMRCA estimates

336 of the single largest CRF01\_AE transmission cluster under different datasets and models  
337 were all close to each other at around the late 1990s to early 2000s, about a decade later  
338 than when the subtype expanded in Southeast Asia coming from Africa [16] and the earliest  
339 identified CRF01\_AE sample in the country around the 1980s [10]. The estimated  
340 evolutionary rates for CRF01\_AE from the BSP and BDSKY analyses were similarly  
341 robust at about 0.003 substitutions/site/year, very close to the estimate in a previous study  
342 when either the full coding region or the *gag* gene is used but not when the *pol* gene or  
343 nearly full-length genome is used [16], [37]. This could be due to different selected regions  
344 in the sequence or different epidemiological dynamics in the sampled locations [56].

345 In our analysis, the confidence intervals of the tMRCA and  $R_e$  of the largest  
346 monophyletic CRF01\_AE and B clusters overlap and thus are comparable or not  
347 significantly different from one another. However, the trend of the CRF01\_AE  $R_e$  was to  
348 always be above that of subtype B except during 2010–2012 when CRF01\_AE  $R_e$   
349 decreased transiently. A recent study in 2022 by Salvaña et al. has shown evidence of  
350 significantly higher viral load in CRF01\_AE infections compared to subtype B and to other  
351 circulating subtypes, which suggests potentially higher transmissibility of CRF01\_AE  
352 infections and a mechanism for why CRF01\_AE has become the predominant subtype in  
353 the Philippines instead of subtype B [9]. The trend of higher CRF01\_AE  $R_e$  in our study is  
354 consistent with the hypothesis of faster transmissibility over subtype B, although further  
355 analysis should be done to confirm these findings. Use of whole genome sequences instead  
356 of subgenomic sequences may lead to more precise estimates of these epidemiological  
357 parameters for each subtype [18] as well as allow for more accurate classification of  
358 subtypes and recombinants forms [17]. The same study by Salvaña et al also suggested

359 higher rates of transmitted drug resistance (TDR) among CRF01\_AE infections compared  
360 to other HIV subtypes, which if confirmed may be a mechanism by which the current  
361 antiretroviral treatment regimens in the country that were tailored for non-CRF01\_AE  
362 epidemics selectively favor the survival and transmission of CRF01\_AE [9]. Another  
363 explanation for the predominance of CRF01\_AE may be due to its being the first to expand  
364 in the local sexually active MSM networks by chance, such as through first-comer  
365 advantage [57]. Both subtypes have been present in the Philippines since the 1980s, but  
366 earlier rapid growth of CRF01\_AE over B was not observed in the country at that time [10].  
367 Both of their largest transmission clusters were introduced prior to 2008 when most cases  
368 were from the heterosexual population [2], but our results suggest that a steep increase in  
369 CRF01\_AE  $R_e$  may have preceded that in B peaking around 2008–2009, shortly after which  
370 cases in the MSM population overtook those in the heterosexual population and during the  
371 rise in cases among 25–34 and 15–24 age groups relative to 35–49 year olds [2]. Consistent  
372 with being the first to expand in the susceptible sexually active MSM population,  
373 CRF01\_AE was found in greater proportion (64%) than B (27%) in a subanalysis of MSM  
374 patients from infections between 2007 and 2012 [10], [11]. One might also speculate that  
375 the period of time wherein public health interventions targeted heterosexual/IDU rather  
376 than MSM risk groups early on in the epidemic may have favored more rapid expansion of  
377 the subtype that spread in the MSM population first if this occurred before policy change  
378 could adapt to the shift in the largest risk group. For example, in the 2009 country report to  
379 the UN Declaration of Commitment to HIV and AIDS, there was a 14% and 55% reach of  
380 prevention programs among the most-at-risk population in female sex workers (FSWs) in  
381 2007 and 2009 compared to 19 and 29% in MSM, respectively [58]. From the same report,



382 there was also a 65 and 65% proportion of condom use among FSWs in 2007 and 2009  
383 compared to 32 and 32% in MSM, respectively [58]. In the HIV epidemic in China, the  
384 infection route of sexual contact was found to be more likely to be an infection with  
385 CRF01\_AE compared to contaminated needles, showing that specific transmission routes  
386 and risk-groups can be dominated by a specific subtype [59]. Transmission in the MSM  
387 risk-group was also found to more likely form clusters [60] and has been linked to more  
388 occurrences of superspreaders than in non-MSM risk groups [61], [62]. Finally, it is also  
389 possible for a combination of multiple factors to have contributed to the predominance of  
390 CRF01\_AE in the Philippines.

391 The CRF01\_AE  $R_e$  declined transiently in 2010–2012, overlapping with the 4th and  
392 5th Philippine AIDS Medium Term Plans developed by the Philippine National AIDS  
393 Council for 2005–2010 [63] and 2011–2016 [58], respectively. Meanwhile, subtype B  $R_e$   
394 reached its first peak, which may have masked any more appreciable decline in cases in this  
395 period. Public health interventions have had a measurable effect on transmission based on  
396 modeling by the Philippine Epidemiology Bureau [1]. Perhaps this is what is reflected in  
397 the fluctuations in  $R_e$ , in particular the shift in the focus of intervention to the MSM risk  
398 group during the 5th AMTP. Further evidence would be needed to confirm this association,  
399 and attribute the decline to specific interventions if not other contributing factors. It must  
400 be mentioned that drug resistance mutation genotyping at RITM was not performed from  
401 2012 to 2013 due to lack of reagents, and neither were there CRF01\_AE sequences from  
402 this time sourced from referring hospitals and social hygiene clinics. Thus, no CRF01\_AE  
403 Philippine sequences from this period were included in this dataset for analysis. It is  
404 possible that undersampling of HIV sequences in this period could affect common ancestor

405 nodes and parameter estimates in the years prior to it. However, the observed dip in  
406 CRF01\_AE  $R_e$  is likely to be genuine since decreases in the proportion of CRF01\_AE cases  
407 relative to subtype B in 2010 and in the absolute counts of CRF01\_AE cases in 2010–2012  
408 were also observed in cohort study data from Telan et al. [11] and visualized by Salvaña et  
409 al. [10]. Additionally, both subtypes exhibited a decrease in  $R_e$  in our analysis, and four (4)  
410 subtype B sequences sampled in 2012 belonging to the large subtype B transmission cluster  
411 were included in the phylodynamic analysis.

412         The peak and decrease in subtype B  $R_e$  on the other hand lagged by a year, again  
413 consistent with cohort study data from Telan et al. [11] and visualized by Salvaña et al. [10]  
414 showing asynchronous peaks and declines of CRF01\_AE and B infections over 2008–2013  
415 [10]. One reason may be a later start of expansion of subtype B in the MSM population  
416 while remaining to make up a large if not dominant proportion in heterosexual/IDU cases  
417 [10], [11]. Perhaps interventions that caused a steep decline in the  $R_e$  of the larger  
418 CRF01\_AE transmission cluster among MSM had a delayed and more gradual effect on the  
419 smaller subtype B transmission cluster spreading in the same susceptible MSM population.  
420 It may also be of interest to investigate whether inter-subtype competition between  
421 CRF01\_AE and B for susceptible hosts played a role in the opposed alternating pattern of  
422 their respective  $R_e$ . A pattern of opposed and alternating oscillation was observed in the  $R_e$   
423 of competing Influenza A virus strains [64].

424         In 2013 onward, the CRF01\_AE  $N_e$  was significantly greater than that of B, which  
425 plateaued since 2009. Additionally, the CRF01\_AE  $R_e$  experienced a steep rebound in  
426 2013, while that of B remained suppressed although not significantly different from each  
427 other given their wide confidence intervals. These agree with the study by Salvaña et al.

428 [10], which showed a rebound and statistically significant shift in the predominant subtype  
429 to CRF01\_AE by 2013. While further investigation on the cause of the rebound is needed,  
430 one suspect that could be considered from our phylogeographic analysis is inter-island  
431 reintroduction of CRF01\_AE such as the Mindanao-to-Luzon transmission we identified  
432 around this time. Continued growth in Philippine island groups/regions outside Luzon/NCR  
433 could also be a factor, given diffuse transmission across locations. Local CRF01\_AE spread  
434 in Visayas increased around this time while that in Luzon and Mindanao remained stable.  
435 Still, other factors may explain the rebound, like behavioral changes facilitated by increased  
436 usage of mobile dating services [65]. It would be interesting to investigate whether this  
437 increased CRF01\_AE  $R_e$  and  $N_e$  in 2013 was simultaneous with the date of increased usage  
438 of mobile dating services in the country. CRF01\_AE  $R_e$  remaining higher than that of B  
439 from 2013 to 2016 could have given CRF01\_AE ample time to grow even more  
440 predominant in the MSM population, reaching 82% of cases since that time [66]. It is  
441 possible that the sequences in this dataset are less informative of  $N_e$  closer to the latest  
442 sample collection date, or that increases in  $R_e$  are not immediately reflected in  $N_e$ . Thus,  
443 analysis with more recent sequences is needed to determine if the rebounded  $R_e$  of subtypes  
444 CRF01\_AE and B after 2013 and 2016, respectively, resulted in continued increases to their  
445 corresponding  $N_e$  soon after.

446 For Luzon, particularly the NCR, to have been inferred the origin of the CRF01\_AE  
447 epidemic is plausible since the most dense and urbanized cities in the Philippines are found  
448 therein. Citizens from various provinces regularly travel to the big cities such as Metro  
449 Manila for work [53], and the busiest and most highly connected airport in the country is in  
450 the NCR [67]. Following this was a complex pattern of diffusion between the three

451 Philippine island groups (13 sampled Philippine regions). The relative rates of migration  
452 between locations could not be concluded to be different from each other, suggesting  
453 uniform import/export of CRF01\_AE infections between island groups. This is also  
454 expected given the extensive interconnectedness and frequent travel of the Filipino  
455 population to and from different island groups/regions in the archipelago [47]. Such a  
456 pattern of CRF01\_AE diffusion suggests the need for geographically wide coverage of  
457 control measures to suppress the overall HIV epidemic in the Philippines. As only limited  
458 samples were sequenced from Visayas and Mindanao relative to Luzon (Supplemental File  
459 XLSX), follow up analysis should be performed using a more uniform sampling of  
460 sequences from all island groups and Philippine regions over time to confirm these findings  
461 as well as achieve higher resolution phylogeography.

462 To summarize, we showed that the introduction of CRF01\_AE into the Philippines  
463 was between the late 1990s and early 2000s, the majority of CRF01\_AE sequences belong  
464 to a single cluster, the CRF01\_AE viral population size  $N_e$  exceeded that of subtype B by  
465 2013, the CRF01\_AE  $R_e$  peaked in 2008–2009 and in 2013 onward, the CRF01\_AE  $R_e$   
466 transiently decreased from 2010 to 2012, the peaks and trough of subtype B  $R_e$  lagged  
467 behind that of CRF01\_AE, CRF01\_AE spread diffusely from Luzon (NCR) to other  
468 Philippine island groups and regions, and CRF01\_AE migration rates between island  
469 groups/regions are comparable with one another. The shift from subtype B to the more  
470 aggressive CRF01\_AE, with its faster progression to advanced immunosuppression [9],  
471 [68] and its implications on treatment and control interventions, greatly highlights the need  
472 to be vigilant on changing phylodynamics of HIV subtypes in the Philippines. Similar  
473 analysis with a more updated dataset should be performed to elucidate how the events from

474 the COVID-19 pandemic from 2020 to 2022 influenced the trajectories of the largest  
475 ongoing HIV-1 transmission clusters in the country. The results of our study characterize  
476 the CRF01\_AE-predominant epidemic, providing context for the effectiveness of past and  
477 current public health measures and may inform future measures toward more effective  
478 control of the HIV epidemic in the Philippines.

479

480

## 481 **Acknowledgements**

482 The authors would like to acknowledge the help of the Epidemiology Bureau of the  
483 Philippine Department of Health for providing access to de-identified metadata from its  
484 national database that were relevant to this study. The authors would also like to thank Hasnat  
485 Sujon for providing valuable technical help in reviewing and improving earlier versions of  
486 the manuscript.

487

## 488 **Data Availability**

489 The datasets and the XML files used in this study can be found at  
490 [https://github.com/mblbdmu/CRF01\\_AE-PH](https://github.com/mblbdmu/CRF01_AE-PH).

491

## 492 **Supplementary Data**

493 Supplementary data contain the parameters used in running BEAST and BEAST2 analyses;  
494 list of HIV subtype CRF01\_AE sequences sampled manually from phylogenetic tree to  
495 estimate CRF01\_AE tMRCA; list of HIV subtype CRF01\_AE sequences sampled uniformly  
496 across date and island group to reconstruct  $N_e$ ,  $R_e$ , and phylogeography; list of HIV subtype  
497 B sequences available for analysis (no subsampling); distribution by island group and region  
498 of uniform subsample of CRF01\_AE sequences; effective reproductive number of HIV  
499 subtype CRF01\_AE and subtype B over time using Birth–Death Skyline analysis; and  
500 submission, sample, and accession IDs of subtype B and CRF01\_AE sequences in the study.

501

## 502 **Funding**

503 This research received no specific grant from any funding agency in the public, commercial,  
504 or not-for-profit sectors.

505

## 506 **Conflicts of Interest**

507 The authors declare that they have no conflicts of interest.

## 508   **References**

- 509   [1]   Epidemiology Bureau DoH, “A Briefer on the Philippine HIV Estimates 2020,” 2020.  
510   [Online]. Available:  
511   [https://doh.gov.ph/sites/default/files/publications/A%20Briefer%20on%20the%20PH](https://doh.gov.ph/sites/default/files/publications/A%20Briefer%20on%20the%20PH%20Estimates%202020_08232021.pdf)  
512   [%20Estimates%202020\\_08232021.pdf](https://doh.gov.ph/sites/default/files/publications/A%20Briefer%20on%20the%20PH%20Estimates%202020_08232021.pdf)
- 513   [2]   Epidemiology Bureau DoH, “HIV/AIDS and ART Registry of the Philippines, June  
514   2022.” Department of Health, 2022. [Online]. Available:  
515   [https://doh.gov.ph/sites/default/files/statistics/EB\\_HARP\\_June\\_AIDSreg2022.pdf](https://doh.gov.ph/sites/default/files/statistics/EB_HARP_June_AIDSreg2022.pdf)
- 516   [3]   Epidemiology Bureau DoH, “HIV/AIDS and ART Registry of the Philippines:  
517   October 2020,” 2020.
- 518   [4]   A. C. Farr and D. P. Wilson, “An HIV epidemic is ready to emerge in the  
519   Philippines.,” *J. Int. AIDS Soc.*, vol. 13, p. 16, Apr. 2010, doi: 10.1186/1758-2652-13-  
520   16.
- 521   [5]   A. G. Ross *et al.*, “HIV epidemic in men who have sex with men in Philippines,”  
522   *Lancet Infect. Dis.*, vol. 13, no. 6, pp. 472–473, Jun. 2013, doi: 10.1016/S1473-  
523   3099(13)70129-4.
- 524   [6]   A. G. P. Ross *et al.*, “The dire sexual health crisis among MSM in the Philippines: an  
525   exploding HIV epidemic in the absence of essential health services.,” *Int. J. Infect.*  
526   *Dis. IJID Off. Publ. Int. Soc. Infect. Dis.*, vol. 37, pp. 6–8, Aug. 2015, doi:  
527   10.1016/j.ijid.2015.06.001.
- 528   [7]   F. J. Paladin, O. T. Monzon, H. Tsuchie, M. R. Aplasca, G. H. J. Learn, and T.  
529   Kurimura, “Genetic subtypes of HIV-1 in the Philippines.,” *AIDS Lond. Engl.*, vol. 12,  
530   no. 3, pp. 291–300, Feb. 1998, doi: 10.1097/00002030-199803000-00007.
- 531   [8]   M. L. Santiago *et al.*, “Molecular epidemiology of HIV-1 infection in the Philippines,  
532   1985 to 1997: transmission of subtypes B and E and potential emergence of subtypes  
533   C and F.,” *J. Acquir. Immune Defic. Syndr. Hum. Retrovirology Off. Publ. Int.*  
534   *Retrovirology Assoc.*, vol. 18, no. 3, pp. 260–269, Jul. 1998, doi: 10.1097/00042560-  
535   199807010-00010.
- 536   [9]   E. M. T. Salvaña *et al.*, “HIV-1 Subtype Shift in the Philippines is Associated With  
537   High Transmitted Drug Resistance, High Viral Loads, and Fast Immunologic  
538   Decline,” *Int. J. Infect. Dis.*, vol. 122, pp. 936–943, Sep. 2022, doi:  
539   10.1016/j.ijid.2022.06.048.
- 540   [10]   E. M. T. Salvaña, B. E. Schwem, P. R. Ching, S. D. W. Frost, S. K. C. Ganchua, and  
541   J. R. Itable, “The changing molecular epidemiology of HIV in the Philippines.,” *Int. J.*  
542   *Infect. Dis. IJID Off. Publ. Int. Soc. Infect. Dis.*, vol. 61, pp. 44–50, Aug. 2017, doi:  
543   10.1016/j.ijid.2017.05.017.
- 544   [11]   E. F. O. Telan *et al.*, “Possible HIV transmission modes among at-risk groups at an  
545   early epidemic stage in the Philippines.,” *J. Med. Virol.*, vol. 85, no. 12, pp. 2057–  
546   2064, Dec. 2013, doi: 10.1002/jmv.23701.
- 547   [12]   E. M. T. Salvaña *et al.*, “High rates of tenofovir failure in a CRF01\_AE-predominant  
548   HIV epidemic in the Philippines.,” *Int. J. Infect. Dis. IJID Off. Publ. Int. Soc. Infect.*  
549   *Dis.*, vol. 95, pp. 125–132, Jun. 2020, doi: 10.1016/j.ijid.2020.02.020.
- 550   [13]   A. Huang *et al.*, “Global Comparison of Drug Resistance Mutations After First-Line  
551   Antiretroviral Therapy Across Human Immunodeficiency Virus-1 Subtypes.,” *Open*

- 552 *Forum Infect. Dis.*, vol. 3, no. 2, p. ofv158, Apr. 2016, doi: 10.1093/ofid/ofv158.
- 553 [14] P. Piot and T. C. Quinn, “Response to the AIDS Pandemic — A Global Health  
554 Model,” *N. Engl. J. Med.*, vol. 368, no. 23, pp. 2210–2218, Jun. 2013, doi:  
555 10.1056/NEJMra1201533.
- 556 [15] Y. Chen *et al.*, “Increased predominance of HIV-1 CRF01\_AE and its recombinants in  
557 the Philippines.,” *J. Gen. Virol.*, vol. 100, no. 3, pp. 511–522, Mar. 2019, doi:  
558 10.1099/jgv.0.001198.
- 559 [16] D. M. Junqueira *et al.*, “New Genomes from the Congo Basin Expand History of  
560 CRF01\_AE Origin and Dissemination,” *AIDS Res. Hum. Retroviruses*, vol. 36, no. 7,  
561 pp. 574–582, Jul. 2020, doi: 10.1089/aid.2020.0031.
- 562 [17] C. Topcu, V. Georgiou, J. H. Rodosthenous, and L. G. Kostrikis, “Comparative HIV-1  
563 Phylogenies Characterized by PR/RT, Pol and Near-Full-Length Genome Sequences,”  
564 *Viruses*, vol. 14, no. 10, p. 2286, Oct. 2022, doi: 10.3390/v14102286.
- 565 [18] G. Dudas and T. Bedford, “The ability of single genes vs full genomes to resolve time  
566 and space in outbreak analysis,” *BMC Evol. Biol.*, vol. 19, no. 1, p. 232, Dec. 2019,  
567 doi: 10.1186/s12862-019-1567-0.
- 568 [19] S. Hué, J. P. Clewley, P. A. Cane, and D. Pillay, “HIV-1 pol gene variation is  
569 sufficient for reconstruction of transmissions in the era of antiretroviral therapy,”  
570 *AIDS*, vol. 18, no. 5, 2004, [Online]. Available:  
571 [https://journals.lww.com/aidsonline/Fulltext/2004/03260/HIV\\_1\\_pol\\_gene\\_variation\\_](https://journals.lww.com/aidsonline/Fulltext/2004/03260/HIV_1_pol_gene_variation_is_sufficient_for.2.aspx)  
572 [is\\_sufficient\\_for.2.aspx](https://journals.lww.com/aidsonline/Fulltext/2004/03260/HIV_1_pol_gene_variation_is_sufficient_for.2.aspx)
- 573 [20] B. T. Foley *et al.*, “HIV Sequence Compendium 2018,” Jun. 2018, doi:  
574 10.2172/1458915.
- 575 [21] S.-Y. Rhee, M. J. Gonzales, R. Kantor, B. J. Betts, J. Ravela, and R. W. Shafer,  
576 “Human immunodeficiency virus reverse transcriptase and protease sequence  
577 database.,” *Nucleic Acids Res.*, vol. 31, no. 1, pp. 298–303, Jan. 2003, doi:  
578 10.1093/nar/gkg100.
- 579 [22] T. F. Liu and R. W. Shafer, “Web resources for HIV type 1 genotypic-resistance test  
580 interpretation.,” *Clin. Infect. Dis. Off. Publ. Infect. Dis. Soc. Am.*, vol. 42, no. 11, pp.  
581 1608–1618, Jun. 2006, doi: 10.1086/503914.
- 582 [23] D. Struck, G. Lawyer, A.-M. Ternes, J.-C. Schmit, and D. P. Bercoff, “COMET:  
583 adaptive context-based modeling for ultrafast HIV-1 subtype identification.,” *Nucleic*  
584 *Acids Res.*, vol. 42, no. 18, p. e144, Oct. 2014, doi: 10.1093/nar/gku739.
- 585 [24] A.-C. Pineda-Peña *et al.*, “Automated subtyping of HIV-1 genetic sequences for  
586 clinical and surveillance purposes: performance evaluation of the new REGA version  
587 3 and seven other tools.,” *Infect. Genet. Evol. J. Mol. Epidemiol. Evol. Genet. Infect.*  
588 *Dis.*, vol. 19, pp. 337–348, Oct. 2013, doi: 10.1016/j.meegid.2013.04.032.
- 589 [25] Los Alamos National Laboratory, “Gene Cutter.” Los Alamos National Laboratory.  
590 Accessed: Feb. 07, 2019. [Online]. Available:  
591 [https://www.hiv.lanl.gov/content/sequence/GENE\\_CUTTER/cutter.html](https://www.hiv.lanl.gov/content/sequence/GENE_CUTTER/cutter.html)
- 592 [26] A. M. Wensing *et al.*, “2017 Update of the Drug Resistance Mutations in HIV-1.,”  
593 *Top. Antivir. Med.*, vol. 24, no. 4, pp. 132–133, Dec. 2016.
- 594 [27] A. Larsson, “AliView: a fast and lightweight alignment viewer and editor for large  
595 datasets.,” *Bioinforma. Oxf. Engl.*, vol. 30, no. 22, pp. 3276–3278, Nov. 2014, doi:  
596 10.1093/bioinformatics/btu531.



- 597 [28] M. N. Price, P. S. Dehal, and A. P. Arkin, “FastTree 2--approximately maximum-  
598 likelihood trees for large alignments.,” *PloS One*, vol. 5, no. 3, p. e9490, Mar. 2010,  
599 doi: 10.1371/journal.pone.0009490.
- 600 [29] B. Q. Minh *et al.*, “IQ-TREE 2: New Models and Efficient Methods for Phylogenetic  
601 Inference in the Genomic Era,” *Mol. Biol. Evol.*, vol. 37, no. 5, pp. 1530–1534, May  
602 2020, doi: 10.1093/molbev/msaa015.
- 603 [30] A. Rambaut, T. T. Lam, L. Max Carvalho, and O. G. Pybus, “Exploring the temporal  
604 structure of heterochronous sequences using TempEst (formerly Path-O-Gen).,” *Virus  
605 Evol.*, vol. 2, no. 1, p. vew007, Jan. 2016, doi: 10.1093/ve/vew007.
- 606 [31] R. Bouckaert *et al.*, “BEAST 2.5: An advanced software platform for Bayesian  
607 evolutionary analysis.,” *PLoS Comput. Biol.*, vol. 15, no. 4, p. e1006650, Apr. 2019,  
608 doi: 10.1371/journal.pcbi.1006650.
- 609 [32] A. J. Drummond, A. Rambaut, B. Shapiro, and O. G. Pybus, “Bayesian coalescent  
610 inference of past population dynamics from molecular sequences.,” *Mol. Biol. Evol.*,  
611 vol. 22, no. 5, pp. 1185–1192, May 2005, doi: 10.1093/molbev/msi103.
- 612 [33] R. R. Bouckaert and A. J. Drummond, “bModelTest: Bayesian phylogenetic site  
613 model averaging and model comparison.,” *BMC Evol. Biol.*, vol. 17, no. 1, p. 42, Feb.  
614 2017, doi: 10.1186/s12862-017-0890-6.
- 615 [34] S. C. Dalai *et al.*, “Evolution and molecular epidemiology of subtype C HIV-1 in  
616 Zimbabwe.,” *AIDS Lond. Engl.*, vol. 23, no. 18, pp. 2523–2532, Nov. 2009, doi:  
617 10.1097/QAD.0b013e3283320ef3.
- 618 [35] G. M. Jenkins, A. Rambaut, O. G. Pybus, and E. C. Holmes, “Rates of molecular  
619 evolution in RNA viruses: a quantitative phylogenetic analysis.,” *J. Mol. Evol.*, vol.  
620 54, no. 2, pp. 156–165, Feb. 2002, doi: 10.1007/s00239-001-0064-3.
- 621 [36] M. Jung *et al.*, “The origin and evolutionary history of HIV-1 subtype C in Senegal.,”  
622 *PloS One*, vol. 7, no. 3, p. e33579, 2012, doi: 10.1371/journal.pone.0033579.
- 623 [37] J. Á. Patiño-Galindo and F. González-Candelas, “The substitution rate of HIV-1  
624 subtypes: a genomic approach.,” *Virus Evol.*, vol. 3, no. 2, p. vex029, Jul. 2017, doi:  
625 10.1093/ve/vex029.
- 626 [38] A. J. Drummond, S. Y. W. Ho, M. J. Phillips, and A. Rambaut, “Relaxed  
627 phylogenetics and dating with confidence.,” *PLoS Biol.*, vol. 4, no. 5, p. e88, May  
628 2006, doi: 10.1371/journal.pbio.0040088.
- 629 [39] N. Lartillot and H. Philippe, “Computing Bayes factors using thermodynamic  
630 integration.,” *Syst. Biol.*, vol. 55, no. 2, pp. 195–207, Apr. 2006, doi:  
631 10.1080/10635150500433722.
- 632 [40] W. Xie, P. O. Lewis, Y. Fan, L. Kuo, and M.-H. Chen, “Improving marginal  
633 likelihood estimation for Bayesian phylogenetic model selection.,” *Syst. Biol.*, vol. 60,  
634 no. 2, pp. 150–160, Mar. 2011, doi: 10.1093/sysbio/syq085.
- 635 [41] M. A. Suchard, P. Lemey, G. Baele, D. L. Ayres, A. J. Drummond, and A. Rambaut,  
636 “Bayesian phylogenetic and phylodynamic data integration using BEAST 1.10,” *Virus  
637 Evol.*, vol. 4, no. 1, Jan. 2018, doi: 10.1093/ve/vey016.
- 638 [42] A. J. Drummond and A. Rambaut, “BEAST: Bayesian evolutionary analysis by  
639 sampling trees.,” *BMC Evol. Biol.*, vol. 7, p. 214, Nov. 2007, doi: 10.1186/1471-2148-  
640 7-214.
- 641 [43] M. D. Hall, M. E. J. Woolhouse, and A. Rambaut, “The effects of sampling strategy

- 642 on the quality of reconstruction of viral population dynamics using Bayesian skyline  
643 family coalescent methods: A simulation study.,” *Virus Evol.*, vol. 2, no. 1, p.  
644 vew003, Jan. 2016, doi: 10.1093/ve/vew003.
- [44] A. Hidano and M. C. Gates, “Assessing biases in phylodynamic inferences in the  
645 presence of super-spreaders,” *Vet. Res.*, vol. 50, no. 1, p. 74, Sep. 2019, doi:  
646 10.1186/s13567-019-0692-5.  
647
- [45] T. Stadler, D. Kühnert, S. Bonhoeffer, and A. J. Drummond, “Birth-death skyline plot  
648 reveals temporal changes of epidemic spread in HIV and hepatitis C virus (HCV).,”  
649 *Proc. Natl. Acad. Sci. U. S. A.*, vol. 110, no. 1, pp. 228–233, Jan. 2013, doi:  
650 10.1073/pnas.1207965110.  
651
- [46] L. Du Plessis, (2018) bdskytools [Source code].  
652 <https://github.com/laduplessis/bdskytools>.  
653
- [47] P. McAdam, (2017) Perform Slatkin Maddison Test on for Trait Transition Across  
654 Phylogeny [Source code]. <https://github.com/prmac/slatkin.maddison>.  
655
- [48] J. Parker, A. Rambaut, and O. G. Pybus, “Correlating viral phenotypes with  
656 phylogeny: accounting for phylogenetic uncertainty,” *Infect. Genet. Evol. J. Mol.*  
657 *Epidemiol. Evol. Genet. Infect. Dis.*, vol. 8, no. 3, pp. 239–246, May 2008, doi:  
658 10.1016/j.meegid.2007.08.001.  
659
- [49] F. Bielejec, G. Baele, B. Vrancken, M. A. Suchard, A. Rambaut, and P. Lemey,  
660 “Spread3: Interactive Visualization of Spatiotemporal History and Trait Evolutionary  
661 Processes,” *Mol. Biol. Evol.*, vol. 33, no. 8, pp. 2167–2169, Aug. 2016, doi:  
662 10.1093/molbev/msw082.  
663
- [50] J. Faeldon, (2020) Philippines Administrative Boundaries JSON Maps [Source code].  
664 <https://github.com/faeldon/philippines-json-maps/tree/master/geojson/regions/lowres>.  
665
- [51] A. Rambaut, A. J. Drummond, D. Xie, G. Baele, and M. A. Suchard, “Posterior  
666 Summarization in Bayesian Phylogenetics Using Tracer 1.7.,” *Syst. Biol.*, vol. 67, no.  
667 5, pp. 901–904, Sep. 2018, doi: 10.1093/sysbio/syy032.  
668
- [52] Rambaut, A., “FigTree v1.3.1.” 2010. [Online]. Available:  
669 <http://tree.bio.ed.ac.uk/software/figtree/>  
670
- [53] T. G. Vaughan, “IcyTree: rapid browser-based visualization for phylogenetic trees and  
671 networks,” *Bioinforma. Oxf. Engl.*, vol. 33, no. 15, pp. 2392–2394, Aug. 2017, doi:  
672 10.1093/bioinformatics/btx155.  
673
- [54] G. Yu, D. K. Smith, H. Zhu, Y. Guan, and T. T. Lam, “ggtree : an r package for  
674 visualization and annotation of phylogenetic trees with their covariates and other  
675 associated data,” *Methods Ecol. Evol.*, vol. 8, no. 1, pp. 28–36, Jan. 2017, doi:  
676 10.1111/2041-210X.12628.  
677
- [55] H. Wickham, *ggplot2*. Cham: Springer International Publishing, 2016. doi:  
678 10.1007/978-3-319-24277-4.  
679
- [56] S. O. Scholle, R. J. F. Ypma, A. L. Lloyd, and K. Koelle, “Viral substitution rate  
680 variation can arise from the interplay between within-host and epidemiological  
681 dynamics,” *Am. Nat.*, vol. 182, no. 4, pp. 494–513, Oct. 2013, doi: 10.1086/672000.  
682
- [57] B. Ferdinandy, E. Mones, T. Vicsek, and V. Müller, “HIV Competition Dynamics  
683 over Sexual Networks: First Comer Advantage Conserves Founder Effects,” *PLOS*  
684 *Comput. Biol.*, vol. 11, no. 2, p. e1004093, Feb. 2015, doi:  
685 10.1371/journal.pcbi.1004093.  
686

- 687 [58] Department of Health (DOH) - Philippines, “5th AIDS Medium Term Plan: 2011-  
688 2016 Philippine Strategic Plan on HIV and AIDS.” Philippine National AIDS  
689 Council, 2011.
- 690 [59] Y. Zhang *et al.*, “Dominance of HIV-1 Subtype CRF01\_AE in Sexually Acquired  
691 Cases Leads to a New Epidemic in Yunnan Province of China,” *PLoS Med.*, vol. 3,  
692 no. 11, p. e443, Nov. 2006, doi: 10.1371/journal.pmed.0030443.
- 693 [60] M. Otani *et al.*, “Phylogenetic analysis reveals changing transmission dynamics of  
694 HIV-1 CRF01\_AE in Japan from heterosexuals to men who have sex with men,” *Int.*  
695 *J. Infect. Dis.*, vol. 108, pp. 397–405, Jul. 2021, doi: 10.1016/j.ijid.2021.05.066.
- 696 [61] X. Li *et al.*, “Nationwide Trends in Molecular Epidemiology of HIV-1 in China,”  
697 *AIDS Res. Hum. Retroviruses*, vol. 32, no. 9, pp. 851–859, Sep. 2016, doi:  
698 10.1089/aid.2016.0029.
- 699 [62] Q. Fan *et al.*, “Analysis of the Driving Factors of Active and Rapid Growth Clusters  
700 Among CRF07\_BC-Infected Patients in a Developed Area in Eastern China,” *Open*  
701 *Forum Infect. Dis.*, vol. 8, no. 3, p. ofab051, Mar. 2021, doi: 10.1093/ofid/ofab051.
- 702 [63] Department of Health (DOH) - Philippines, “4th AIDS Medium Term Plan.”  
703 Philippine National AIDS Council, 2005.
- 704 [64] L. Gatti *et al.*, “Cross-reactive immunity potentially drives global oscillation and  
705 opposed alternation patterns of seasonal influenza A viruses,” *Sci. Rep.*, vol. 12, no. 1,  
706 p. 8883, May 2022, doi: 10.1038/s41598-022-08233-w.
- 707 [65] J. Clark, “Mobile dating apps could be driving HIV epidemic among adolescents in  
708 Asia Pacific, report says,” *BMJ*, p. h6493, Dec. 2015, doi: 10.1136/bmj.h6493.
- 709 [66] E. M. Salvaña *et al.*, “1282. Detection of HIV Transmitted Drug Resistance by Next-  
710 Generation Sequencing in a CRF01\_AE Predominant Epidemic,” *Open Forum Infect.*  
711 *Dis.*, vol. 5, no. Suppl 1, p. S391, Nov. 2018, doi: 10.1093/ofid/ofy210.1115.
- 712 [67] P. Cal, E. Doña, H. Lidasan, and A. B. Manalang, “Airport Location and the Intensity  
713 of Urban Concentration.” Eastern Asia Society for Transportation Studies, 2010. doi:  
714 10.11175/easts.8.2365.
- 715 [68] M. Chu *et al.*, “HIV-1 CRF01\_AE strain is associated with faster HIV/AIDS  
716 progression in Jiangsu Province, China,” *Sci. Rep.*, vol. 7, no. 1, p. 1570, May 2017,  
717 doi: 10.1038/s41598-017-01858-2.  
718
- 719

720 **Figure Legends**

721 **Figure 1.** (A) Maximum likelihood phylogenetic tree of Philippine CRF01\_AE PR/RT  
722 sequences relative to international sequences obtained from the LANL database  
723 reconstructed with IQ-TREE2. The red arrow indicates the node, with SH-aLRT and  
724 UFBoot branch support values, of the most recent common ancestor of the large  
725 monophyletic clade to which the majority of CRF01\_AE sequences belong. This clade is  
726 also emphasized with a blue rectangular highlight. The bottom scale bar shows a reference  
727 branch length for 0.02 substitutions/site. Country abbreviation: AT:Austria; AU:Australia;  
728 CM:Cameroon; CN:China; DK:Denmark; ES:Spain; FI:Finland; FR:France; GB:United  
729 Kingdom; HK:Hong Kong; ID:Indonesia; JP:Japan; KR:South Korea; KW:Kuwait;  
730 MM:Myanmar; MY:Malaysia; PH:Philippines; PK:Pakistan; SE:Sweden; SG:Singapore;  
731 TH:Thailand; TW:Taiwan; US:United States; VN:Vietnam. (B) Root-to-tip plot generated  
732 with TempEst showing a positive correlation between time and divergence or accumulating  
733 mutations among sequences, indicating suitability of sequence data for time-scaled  
734 phylogenetic and phylodynamic analysis. (C) Time-scaled phylogenetic tree generated using  
735 BEAST2 from a manual subset of the monophyletic Philippine CRF01\_AE sequences and  
736 contextual international LANL sequences. The red arrow indicates the node of the most  
737 likely time to the most recent common ancestor for the Philippine CRF01\_AE sequences,  
738 along with an error bar for the uncertainty in estimated time. This clade is also emphasized  
739 with a blue rectangular highlight.

740 **Figure 2.** Phylodynamics of HIV CRF01\_AE in the Philippines measured between mid-  
741 1990s and 2018 reconstructed by BEAST2 analysis of uniformly sampled Philippine  
742 CRF01\_AE PR/RT sequences. (A) Time-scaled maximum clade credibility tree from  
743 BDSKY analysis summarized with TreeAnnotator. Common ancestor nodes are highlighted  
744 as black dots. (B) The change in CRF01\_AE effective population size ( $N_e$ ) over time in log  
745 scale, with the median represented as a black line and the 95% HPD as a blue-shaded interval,  
746 obtained from BSP analysis. (C) The change in the effective reproductive number ( $R_e$ ) over  
747 time, with the mean represented as a black line and the 95% HPD as a blue-shaded interval,  
748 obtained from BDSKY analysis. A dashed red line indicates the value of  $R_e$  equal to 1.  
749

750 **Figure 3.** Analysis of geographic spread and relative migration rates of HIV CRF01\_AE  
751 across Philippine island groups. (A) Maximum clade credibility tree of monophyletic  
752 Philippine CRF01\_AE PR/RT sequences generated with BEAST under the “phylogeog”  
753 model and summarized with TreeAnnotator. Branches are labeled with posterior probability  
754 support values of corresponding nodes and are colored according to the most likely  
755 geographic location of a branch at the level of Philippines island groups: Luzon (red), Visayas  
756 (green), Mindanao (purple), and Mindanao+Luzon (blue). (B) Forest plot with mean and 95%  
757 HPD estimate of the asymmetric relative migration rates of CRF01\_AE between all pairs of  
758 Philippine island groups. A dashed line indicates a relative migration rate equal to 1.0, or no  
759 greater or lesser than other migration rates. (C) Phylogeographic spread of CRF01\_AE  
760 between Luzon, Visayas, and Mindanao island groups over time visualized with SPREAD3.  
761 The size of the red polygons over island groups correspond to the intensity of localized virus  
762 transmission at the specified location and time.

763

764 **Figure 4.** Comparison of phylodynamics between Philippine CRF01\_AE and subtype B. (A)

765 Time-scaled maximum clade credibility tree from BDSKY analysis of subtype B PR/RT

766 sequences summarized with TreeAnnotator. Common ancestor nodes are highlighted as

767 black dots. (B) The change in subtype B effective population size ( $N_e$ ) over time in log scale

768 obtained from BSP analysis, superimposed over that of CRF01\_AE, with the median

769 represented as a black line and the 95% HPD as an orange-shaded interval. (C) The change

770 in the effective reproductive number ( $R_e$ ) over time obtained from BDSKY analysis,

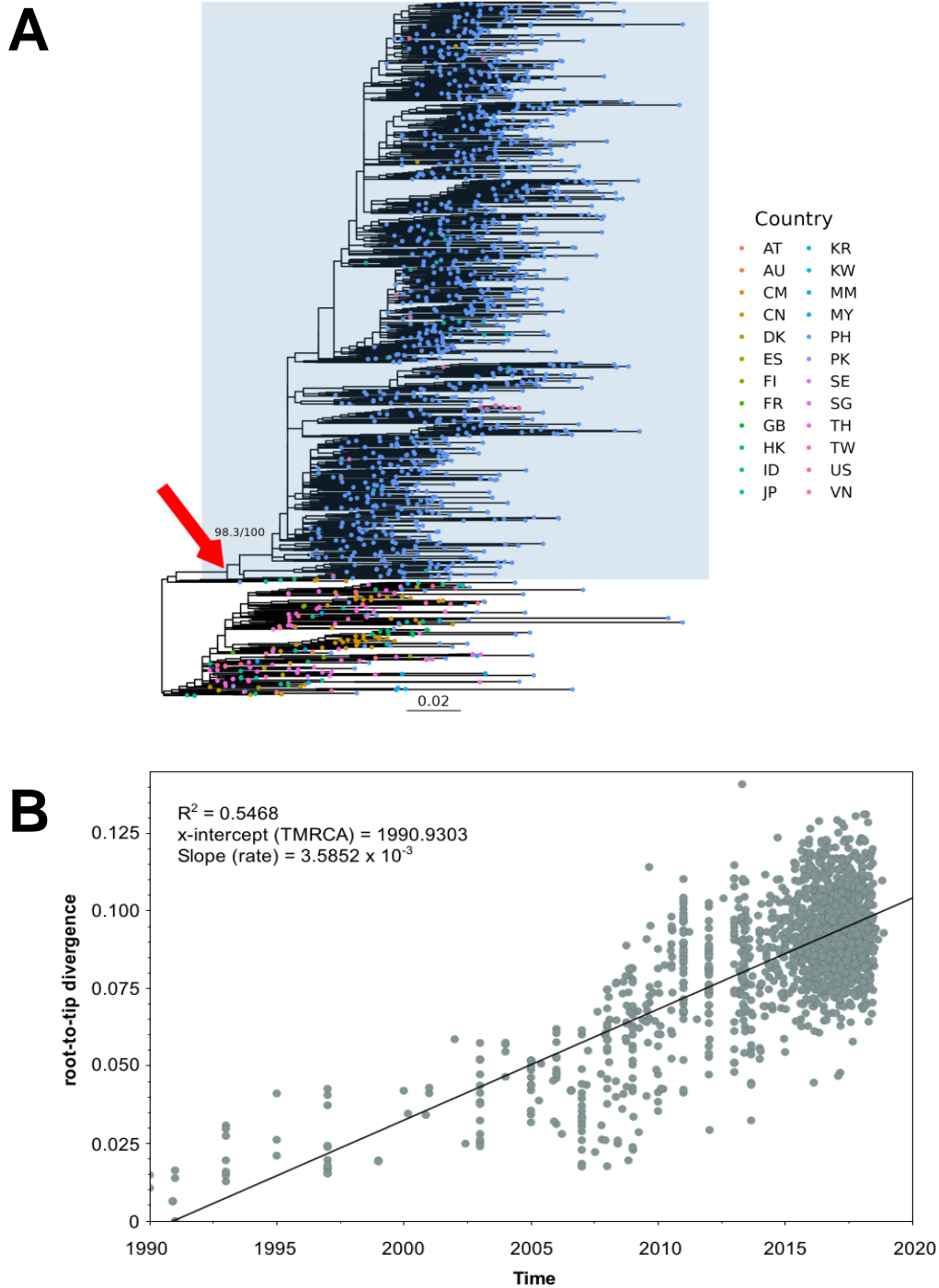
771 superimposed over that of CRF01\_AE, with the mean represented as a black line and the

772 95% HPD as an orange-shaded interval. A dashed red line indicates the value of  $R_e$  equal to

773 1.

774

Figure 1



C

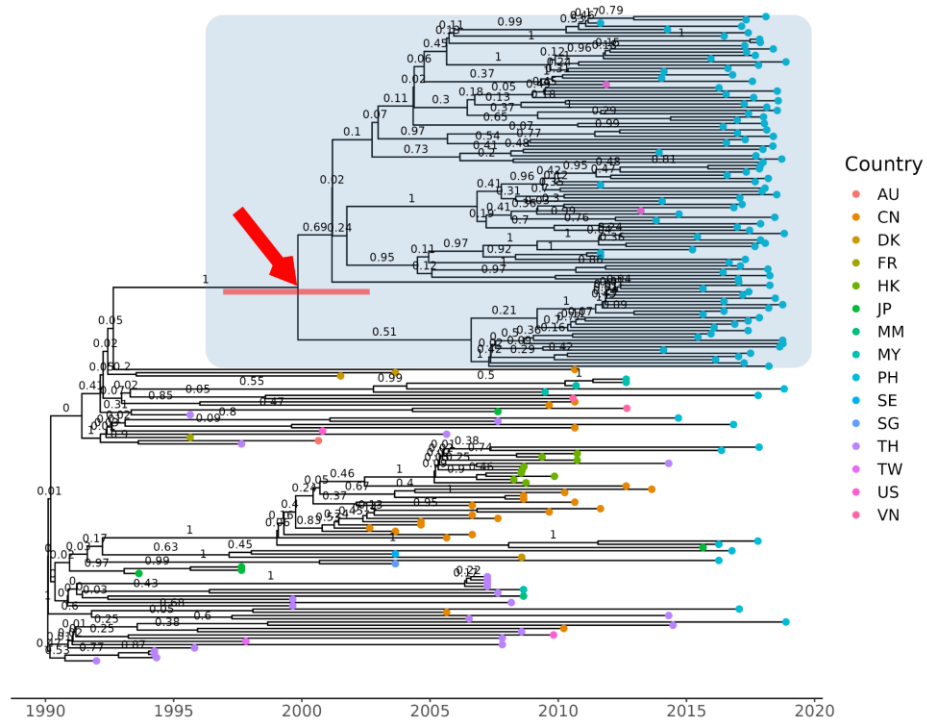
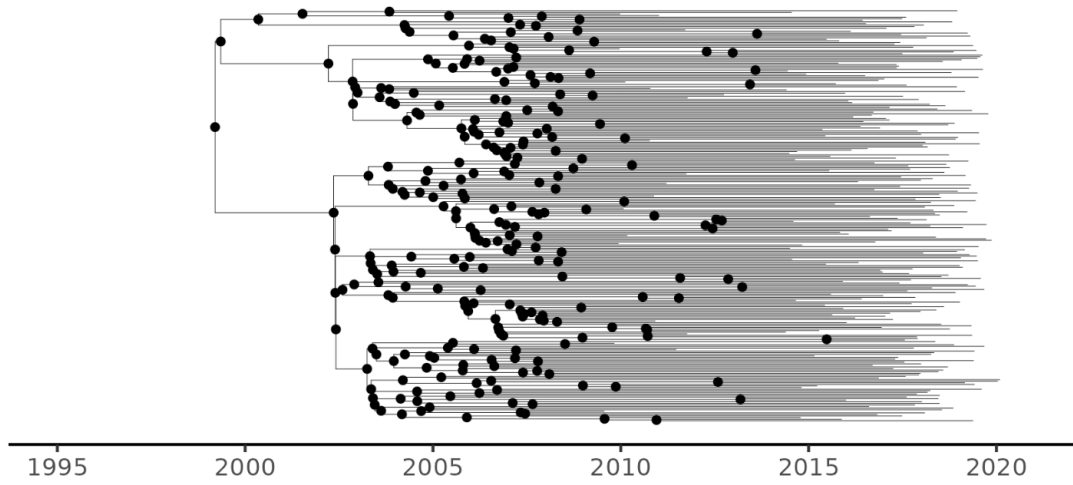


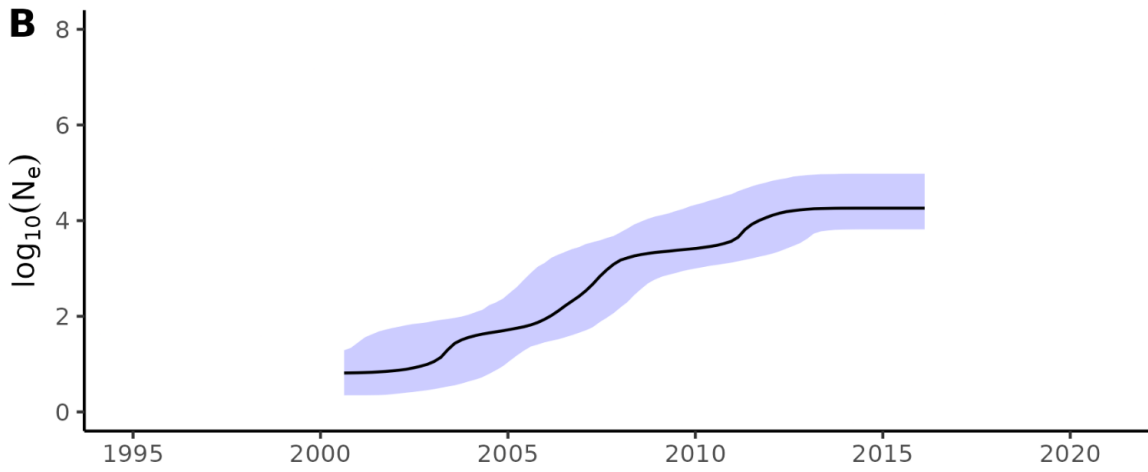


Figure 2

**A**



**B**



**C**

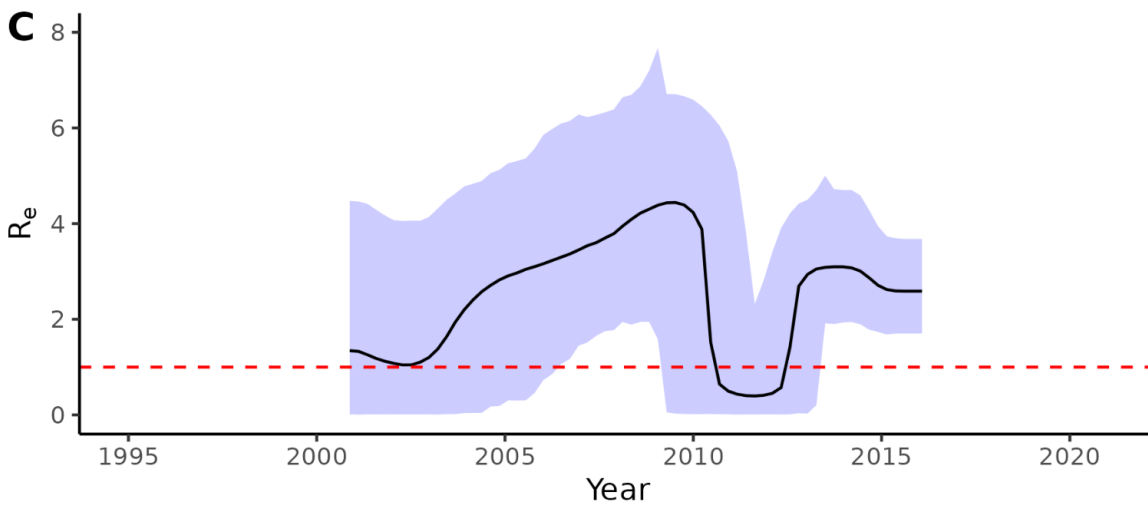


Figure 3

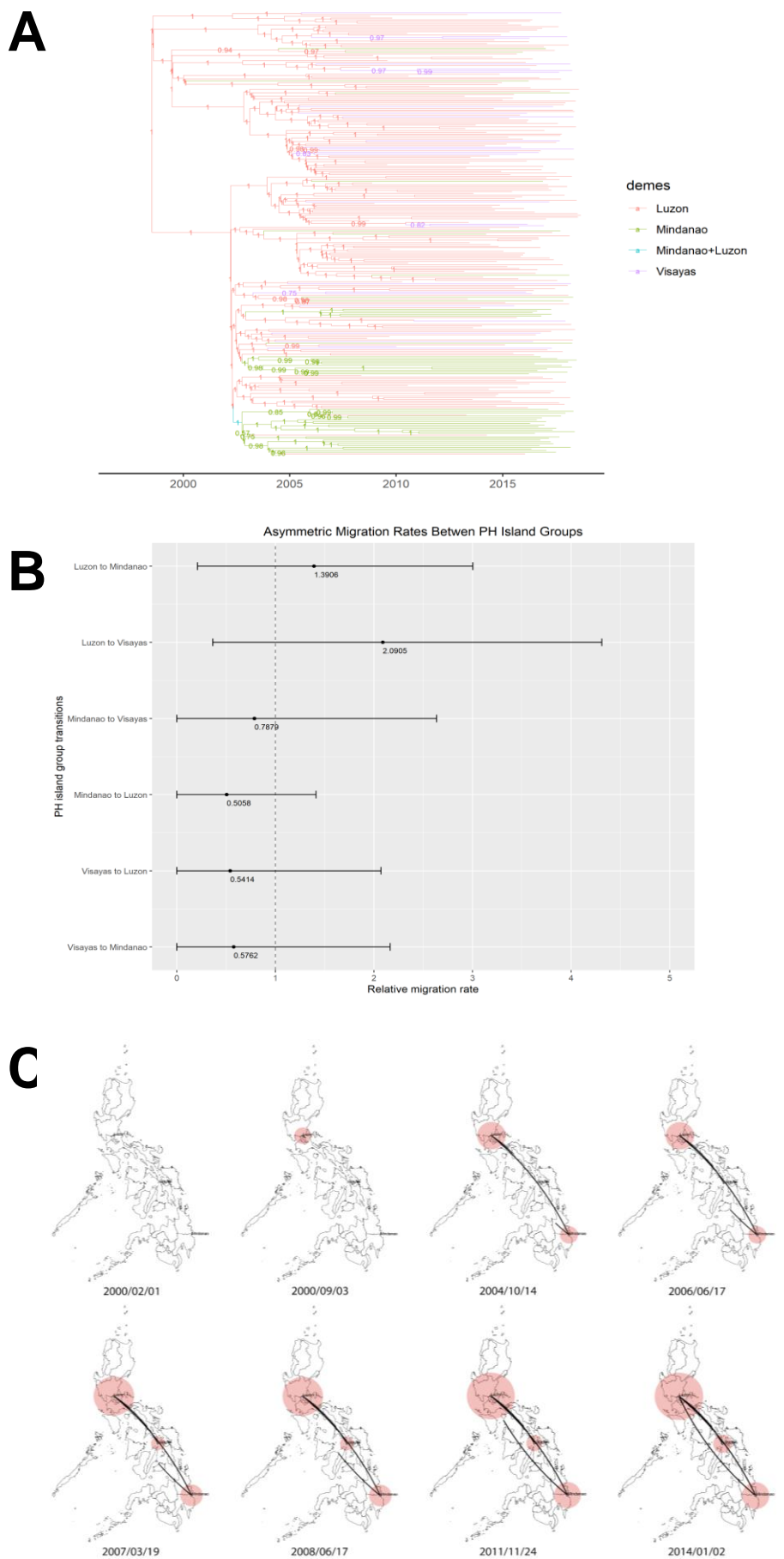
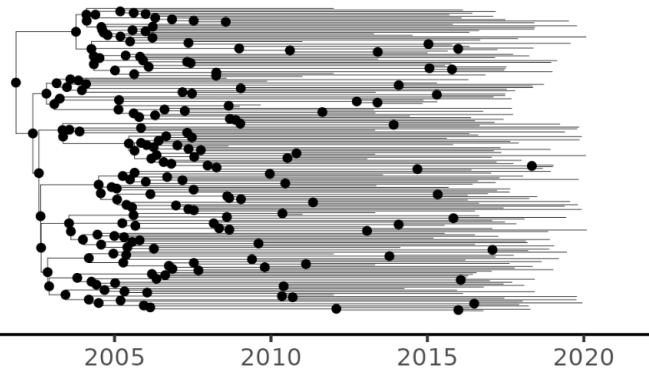
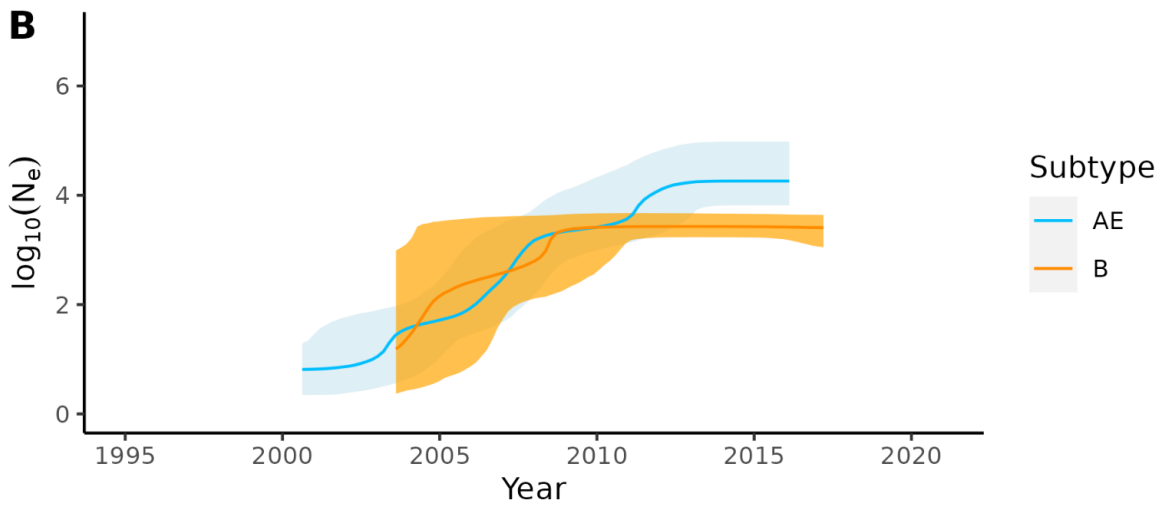


Figure 4

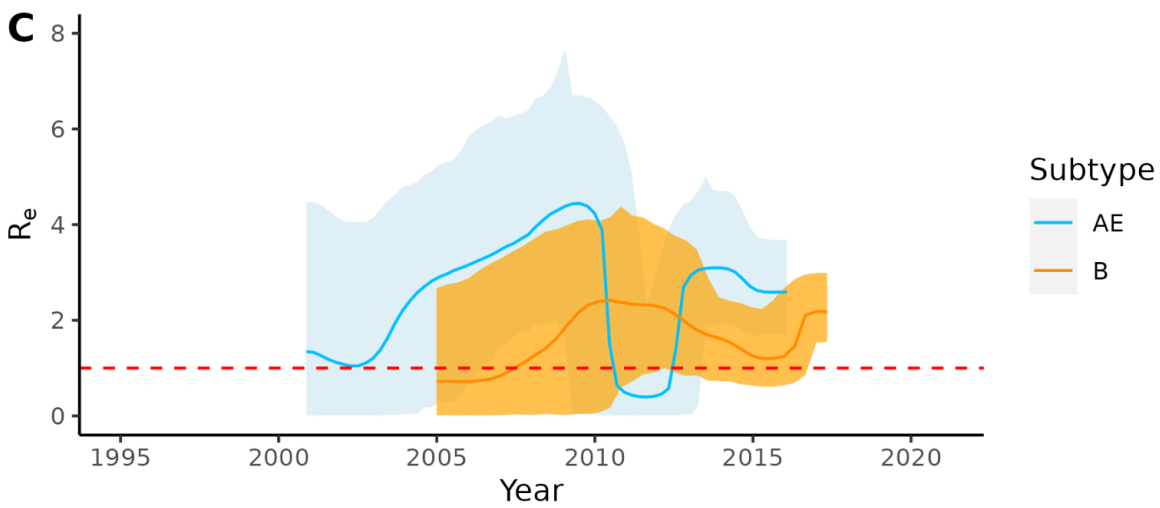
**A**



**B**



**C**



## Reconstructing the phylodynamic history and geographic spread of the CRF01\_AE-predominant HIV-1 epidemic in the Philippines from PR/RT sequences sampled from 2008-2018

### Supplementary Data

### Supplementary Figures

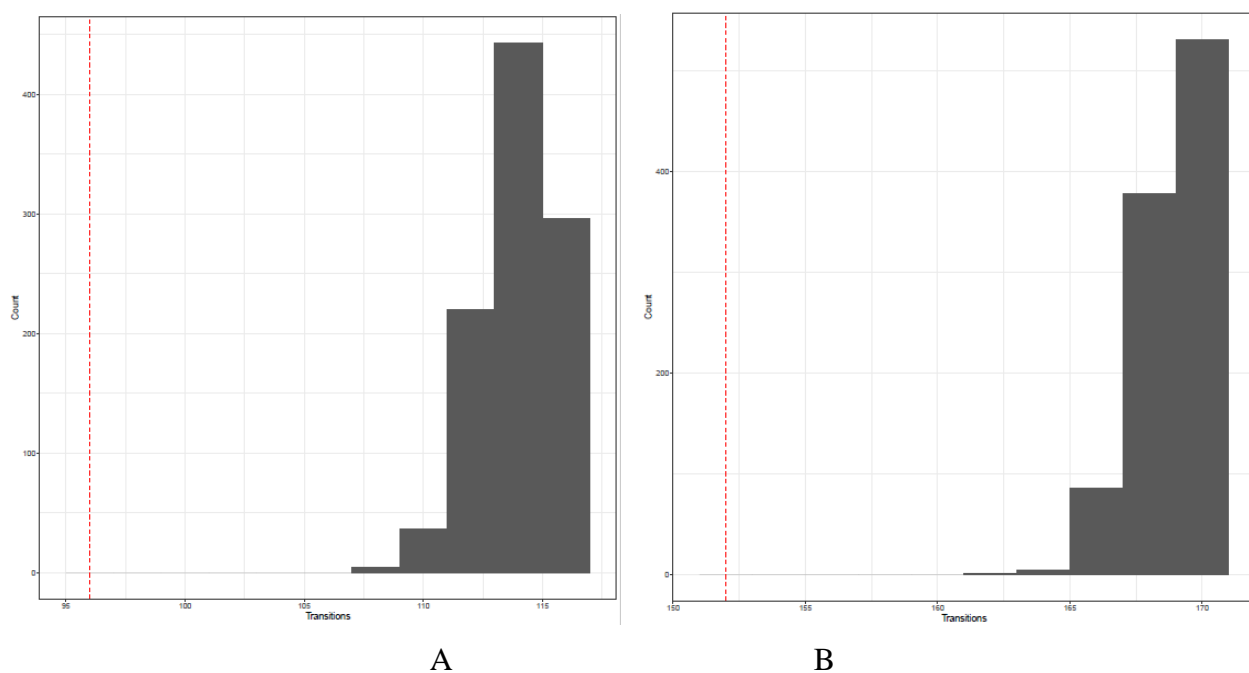


**Figure S1.** Slatkin–Maddison test for geographic clustering using the full set of Philippine CRF01\_AE PR/RT sequences from the large CRF01\_AE transmission cluster by (A) island group and (B) region. The dashed red line indicates the observed number of transitions. The gray histograms depict the distribution of transitions from the null model with 999 replicates.

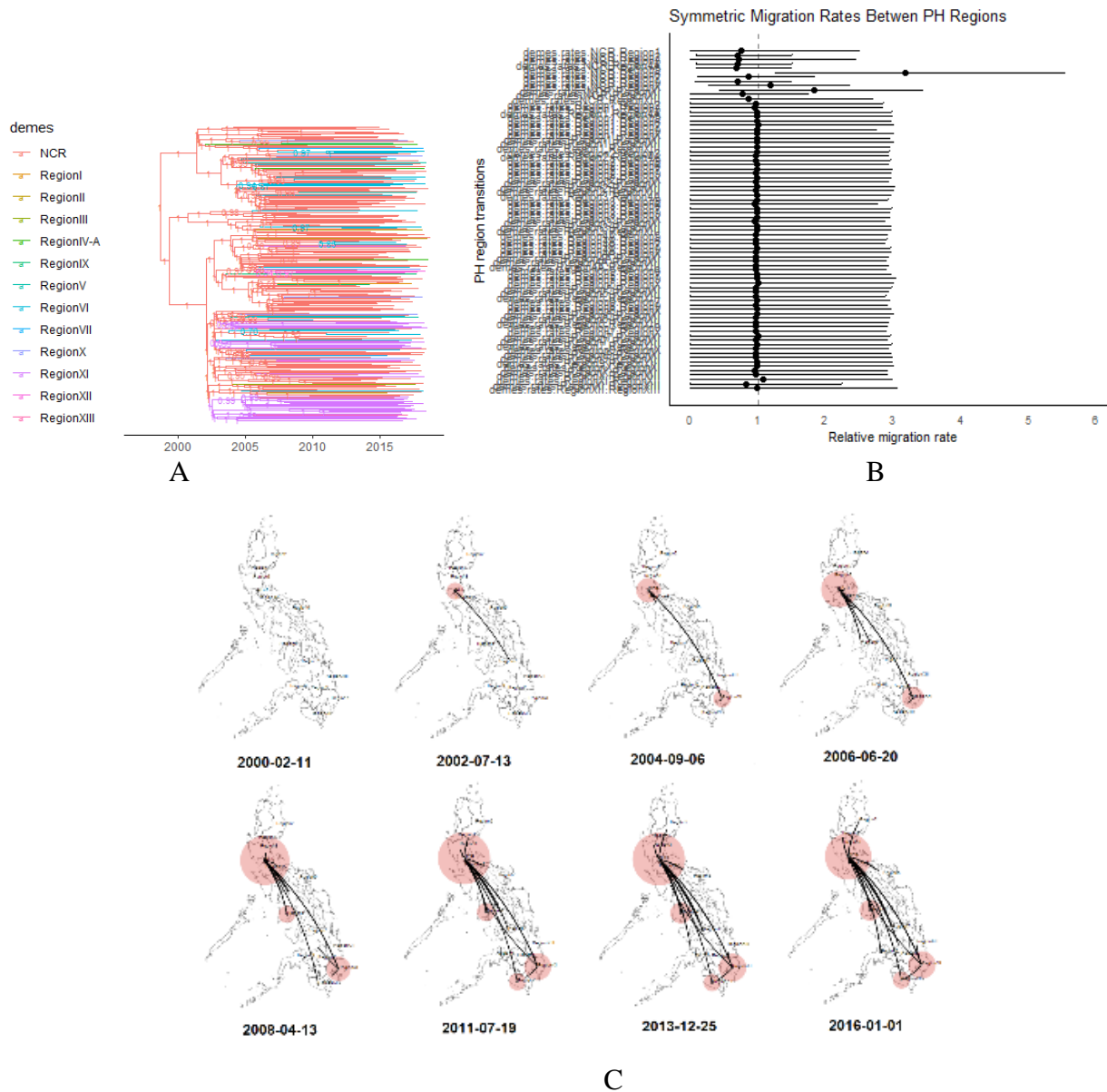


**Figure S2.** Analysis of geographic spread and relative migration rates of HIV CRF01\_AE in the Philippines across PH administrative regions. (a) Maximum clade credibility tree of monophyletic PH CRF01\_AE PR/RT sequences generated with BEAST1 under ‘phyloge’ model and summarized with TreeAnnotator. Branches are labeled with posterior probability support values of corresponding nodes. Branches are colored according to the most likely geographic location of a branch at the level of PH administrative regions, wherein NCR (color red) was the most likely location of origin for the local epidemic followed by spread to other regions. (b) Forest plot of the relative migration rates of CRF01\_AE between all pairs of PH administrative regions with a dashed line indicating a relative migration rate equal to 1.0. The 95% HPD intervals imply that there is no significant difference between the rate of migration of CRF01\_AE between PH administrative regions. This suggests that no subset of migration rates dominate the diffusion process (i.e. no pair of locations that are the primary exporter-importer pair for CRF01\_AE) and that there is extensive mixing between locations. (c) Phylogeographic spread of CRF01\_AE between PH

administrative regions over time visualized with SPREAD3. The size of the red polygons over the regions correspond to the intensity of localized virus transmission at the specified location and time.

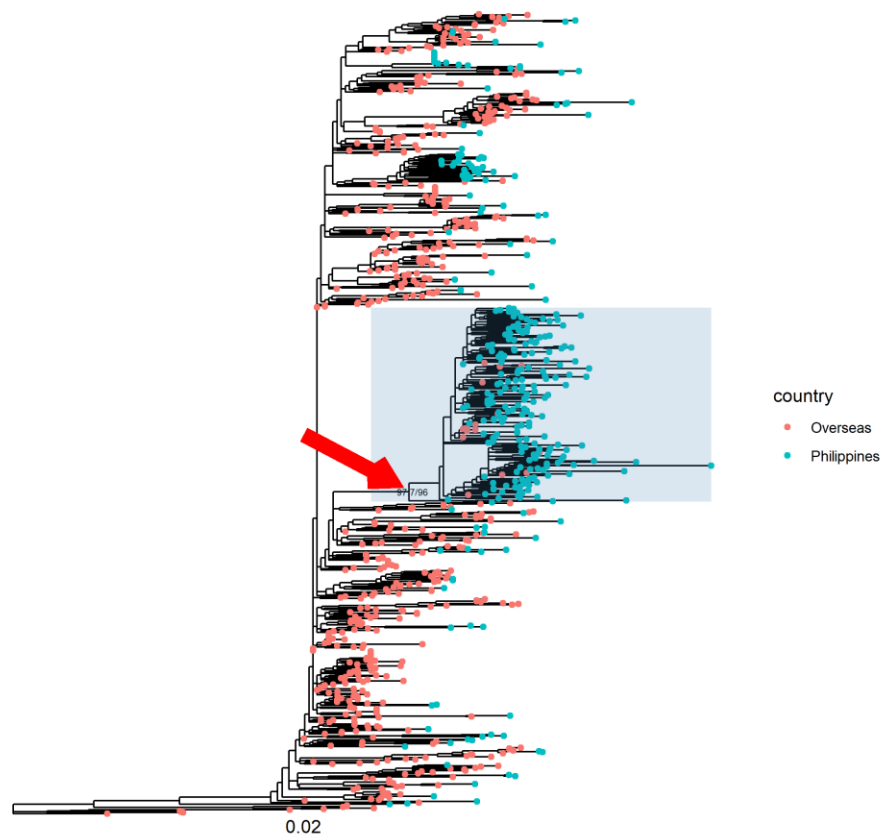


**Figure S3.** Maximum likelihood phylogeny of HIV subtype B generated with IQ-TREE2 using all eligible Philippine subtype B PR/RT sequences from the RITM MBL DRG database with a sampling period from 2008 to 2020, in the context of the closest subtype B sequences retrieved from LANL using HIV-BLAST and subtype C and A outgroup sequences. Tips of Philippines sequences from either the RITM MBL DRG or LANL databases are colored blue while overseas sequences from LANL are colored red. The red arrow indicates the node, with SH-aLRT and UFBoot branch support values, of the most recent common ancestor of the large monophyletic clade to which the majority of Philippine subtype B sequences belong. This clade is also emphasized with a blue rectangular highlight. The bottom scale bar shows a reference branch length for 0.02 substitutions/site. Overseas sequences contained within this cluster included those from Taiwan, Canada, United States, Japan, South Korea, Thailand, Australia.

## Supplementary Tables

**Table S1.** Posterior epidemiological and evolutionary parameter estimates from all BEAST and BEAST2 analyses performed in the study, including the mean and 95% HPD of each parameter under each analysis.

analysis / model / software	tMRCA analysis / Coalescent Bayesian Skyline / BEAST2	Phylodynamics / Coalescent Bayesian Skyline / BEAST2		Phylodynamics / Birth-Death Skyline Serial / BEAST2		Phylogeography / Coalescent Bayesian Skyline / BEAST
HIV subtype	CRF01_AE	CRF01_AE	B	CRF01_AE	B	CRF01_AE
subsampling / sequences	manual / PH largest monophyletic + international	uniform-island group / PH largest monophyletic	NA / PH largest monophyletic	uniform-island group / PH largest monophyletic	NA / PH largest monophyletic	uniform-island group / PH largest monophyletic
<b>tMRCA of largest monophyletic PH clade</b>	1999.2027 [95% HPD: 1996.2853, 2001.9984]	1996.8085 [95% HPD: 1992.6457, 2000.6302]	1995.1435 [95% HPD: 1982.4503, 2003.6044]	1997.9899 [95% HPD: 1995.0292, 2000.888]	2001.0256 [95% HPD: 1995.091, 2004.9955]	1998.5122 [95% HPD: 1994.9761, 2001.5033]
<b>clock rate (strict ucl)</b>	2.413E-3 [95% HPD: 2.0457E-3, 2.7851E-3]	2.7204E-3 [95% HPD: 2.2991E-3, 3.1225E-3]	2.524E-3 [95% HPD: 1.8829E-3, 3.1806E-3]	2.8037E-3 [95% HPD: 2.4367E-3, 3.1644E-3]	2.89E-3 [95% HPD: 2.36E-3, 3.41E-3]	2.9214E-3 [95% HPD: 2.4574E-3, 3.381E-3]
<b>clock rate std dev (ucl)</b>	0.4135 [95% HPD: 0.3119, 0.5204]	NA	0.4512 [95% HPD: 0.3479, 0.54]	NA	0.475 [95% HPD: 0.382, 0.566]	NA
<b>origin of the epidemic</b>	NA	NA	NA	1994.5544 [95% HPD: 1992.6878, 1998.2369]	1991.5307 [95% HPD: 1988.2588, 1994.8316]	NA
<b>becomeUninfectious rate</b>	NA	NA	NA	0.3315 [95% HPD: 0.1857, 0.5058]	0.572 [95% HPD: 0.343, 0.8163]	NA
<b>sampling proportion</b>	NA	NA	NA	3.2456E-3 [95% HPD: 1.2577E-3, 5.1211E-3]	3.94E-3 [95% HPD: 2.06E-3, 5.66E-3]	NA

**Table S2.** BaTS analysis using island group as trait, 1000 trees downsampled from the CRF01\_AE BSP sampled trees, and 999 simulated null trees.

Statistic	observed.mean	lower.95..CI	upper.95..CI	null.mean	lower.95..CI.1	upper.95..CI.1	significance
AI	9.14	7.82	10.45	14.00	12.86	15.08	<b>&lt;0.001</b>
PS	54.35	50.00	58.00	72.14	69.33	74.42	<b>&lt;0.001</b>
MC (Luzon)	13.39	11.00	17.00	7.92	6.44	10.29	<b>0.014</b>
MC (Visayas)	2.56	2.00	3.00	1.66	1.21	2.08	<b>0.002</b>
MC (Mindanao)	4.75	4.00	6.00	2.31	1.96	3.05	<b>0.001</b>